J. of Electromagn. Waves and Appl., Vol. 26, 294–306, 2012

A NEW MULTIPLE-BEAM FORMING NETWORK DESIGN APPROACH FOR A PLANAR ANTENNA ARRAY USING CORPS

A. Arce[1,*], D. H. Covarrubias[1], M. A. Panduro[2], and L. A. Garza[2]

[1]Electronics and Telecommunications Department, CICESE Research Centre, Carretera Ensenada-Tijuana 3918, Ensenada 22860, Mexico

[2]Unidad Acadmica Multidisciplinaria Reynosa-Rodhe, Universidad Autnoma de Tamaulipas (UAT), Carretera Reynosa-San Fernando, Reynosa, Tamaulipas 8879, Mexico

Abstract—This paper deals with a novel way to design and analyze beam-forming networks (BFNs) for a multi-beam steerable planar antenna array using Coherently Radiating Periodic Structures (CORPS) technology. A 9-beam design of CORPS-BFN configuration with aperture reuse and with a innovative way to feed it is proposed and analyzed. In this design, the complex inputs of the feeding network are optimized using the well-known method of Genetic Algorithms (GA). Simulation results reveal interesting characteristics in the array factor response for the multi-beam steerable planar array. Furthermore, a significant simplification of the feeding network for a planar array based on CORPS is achieved, improving the results of literature dealing with different CORPS-BFN configurations and antenna array geometries.

1. INTRODUCTION

Current and future applications require essential characteristics of antenna systems such as the ability to redirect and reorganize its services efficiently together with the ability to handle multiple independent beams. These features are combined effectively in multiple-beam forming networks (M-BFN).

There are different alternatives to use a M-BFN. This work presents the technological concept of coherently radiating periodic

Received 14 December 2011, Accepted 10 January 2012, Scheduled 19 January 2012

* Corresponding author: Armando Arce (arce@cicese.edu.mx).

structures (CORPS) [1–3] applied into BFN for a planar antenna array, in order to design a multiple-beam forming network.

With new design philosophies, CORPS technological concept is introduced and first applied directly to radiating elements [4]. The methodology to implement CORPS technology as a beam-forming network for a phased array was proposed in [1]. The design of BFN for scannable multi-beam arrays using CORPS was presented in [2, 3] using a linear array and in [5] with circular geometry. Other recent research work is focus in using CORPS-BFN in specific applications and in the development of evolutions to improve efficiency [6].

The simplification of the network has been tackled in [2, 3] and [5], and the final results revealed a significant simplification of the feeding network specially in the circular array geometry using CORPS and evolutionary computation. However, the concept of CORPS for scannable multi-beam bi-dimensional arrays and the study of new structures for designing BFN can be focused on design cases where the simplification and performance of the feeding network can be improved.

This research work, based on the unique features of CORPS technology, will introduce a innovative way to analyze the design of a feeding network for scannable multi-beam planar antenna arrays. In this way, the main objective of this paper is to define a BFN using CORPS principles and the method of GA [7–13] to optimize the required amplitude and phase excitations that should be introduced to the network, in order to generate a scannable multi-beam planar array.

The main contribution of this work is presenting a new perspective in the design of CORPS-BFN considering scannable multi-beam planar arrays with optimized inputs.

The paper is organized as follows. Section 2 describes the CORPS ideal behavior implemented as a BFN followed by a description of the optimization process applied. The simulation set up and results are presented in Section 3. Finally, conclusions of this work are presented in Section 4.

2. THEORETICAL STUDY

2.1. CORPS-BFN Model

CORPS-BFN model previously introduced in [4] is based on the basic principles of behavior of periodic structures called CORPS. A CORPS-BFN is implemented using identical unit cells as a basic node to form a entire feeding network, as described in [1]. This unit cell can act as power splitter (Split (S)-node) or power combiner (Recombination(R)-node) by changing its relative position as shown in Fig. 1.

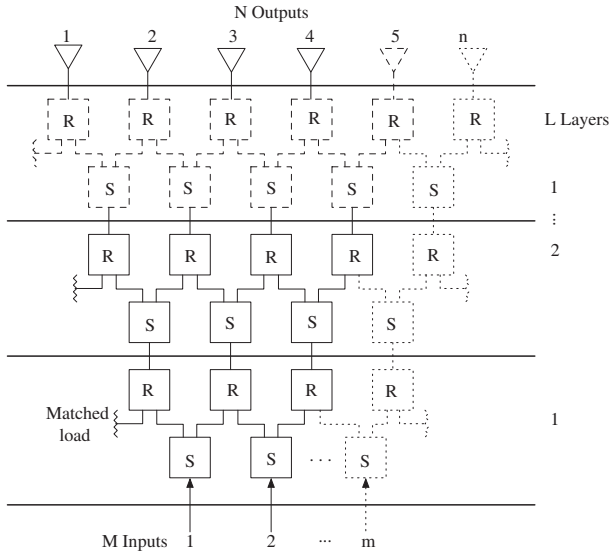

Figure 1. Schematic of CORPS beam-forming network with S and R nodes of M inputs, N outputs and L layers.

The unit cell can be represented as a 3-port component characterized by the following scattering matrix [1]:

$$[S]_{\text{cell}} = \frac{j}{\sqrt{2}} \begin{bmatrix} 0 & 1 & 1 \\ 1 & 0 & 0 \\ 1 & 0 & 0 \end{bmatrix} \tag{1}$$

The ideal matrix in (1) ensures that the basic component is perfectly matched and isolated, and therefore there is no interaction between input signals. Subsequently, a complete feeding network can be formed iteratively, alternating S and R nodes, as shown in Fig. 1.

The schematic of CORPS-BFN in Fig. 1 shows that it is feasible to establish several configurations with different inputs, outputs and layers that handle multiple orthogonal beams simultaneously according to the application. Typically, output ports (N) are greater than input ports (M).

In order to calculate the fields at the output of each unit cell $[V^-]_{\text{cell}} = [V_1^- V_2^- V_3^-]^T$ in (1) we can use:

$$\begin{bmatrix} V_1^- \\ V_2^- \\ V_3^- \end{bmatrix}_{\text{cell}} = \begin{bmatrix} S_{11} & S_{12} & S_{13} \\ S_{21} & S_{22} & S_{23} \\ S_{31} & S_{32} & S_{33} \end{bmatrix}_{\text{cell}} \cdot \begin{bmatrix} V_1^+ \\ V_2^+ \\ V_3^+ \end{bmatrix}_{\text{cell}} \tag{2}$$

where $[S]_{\text{cell}} = [S_{11} \ldots S_{33}]^T$ is the scattering matrix of a unit cell, and $[V^+]_{\text{cell}} = [V_1^+ V_2^+ V_3^+]^T$ is the complex excitation (amplitude and

phase) at the input ports of a unit cell. If we evaluate (2) and interconnect a feeding network as in Fig. 1, we can simulate and analyze a beam-forming network that uses CORPS technology which can be physically implemented, as in [1, 6].

At the top of the feeding network, we must consider the geometry used on the antenna array. In our case, we consider an equidistant planar array of $N \times N$ antenna elements (two dimensions). For simplicity, consider the planar array to be made of omni-directional antenna elements. Its array factor for a set of complex inputs [**a**] feeding CORPS-BFN is given by the next equation [15]:

$$AF(\theta, \varphi, \mathbf{a}) = \sum_{i=1}^{N} \sum_{j=1}^{N} a_{ij} \exp[jk(x_{ij} \sin\theta \cos\varphi) + (y_{ij} \sin\theta \sin\varphi)] \quad (3)$$

where a_{ij} represents the complex excitation of the ijth antenna element of the array considering the the feeding network, x_{ij} and y_{ij} the position of the ijth element of the array, θ and φ the angle of incidence in the elevation and azimuth plane respectively, and $k = 2\pi/\lambda$ the phase constant, where λ is the signal wavelength.

The complex inputs feeding the CORPS network are taken into account in the array factor considering the proposed inputs (i.e., the complex excitation to feed the ijth radiator of the array) and a progressive phase excitation, given by:

$$a = A_{ij} \exp(j\xi_{ij}) \exp(j\psi_{ij}) \qquad \text{for } 1 \leq i \leq M \quad 1 \leq j \leq M \qquad (4)$$

The first term $A_{ij} \exp(j\xi_{ij})$ in (4) denotes the typical complex excitation (amplitude and phase, respectively) where $\xi_{ij} \in [0, 180]$, and the second term $\exp(j\psi_{ij})$ adds a phase excitation in the complex inputs of the feeding network and related to a linear interpolation of a conventional progressive phase excitation. The purpose of establishing this phase excitation is that the optimization process searches possible phase perturbations that generate a near-optimal array factor with angles of the main beam near to the direction of interest. Finally, M represents the number of input ports of the network that electronically control the radiation pattern, and the term ψ_{ij} in the exponential is:

$$\psi_{ij} = k[xm_{ij} \sin\theta_0 \sin\varphi_0 + ym_{ij} \sin\theta_0 \cos\varphi_0] \qquad (5)$$

In (5), (θ_0, φ_0) indicate the direction of maximum radiation, and the term xm_{ij} and ym_{ij} are given by:

$$xm_{ij} = x_{ij} + (x/L)(i-1) \qquad ym_{ij} = y_{ij} \cos(\theta/L) \qquad (6)$$

where L is the total number of layers of the CORPS-BFN system.

The optimization process followed to obtain near-optimal solutions to the complex inputs to feed the network is described in the next subsection.

2.2. Optimization Process

The optimization process applied to the CORPS-BFN system is used to obtain complex excitations (amplitudes and phases) that should be directly applied at the input ports of the feeding network. In this paper, these excitations are determined by a robust and well-known heuristic technique, called genetic algorithms.

By analogy with the process of natural selection and evolution, in GA the set of parameters to be optimized (genes) defines an individual or potential solution X (chromosome). A collection of individuals form the population, which evolves through 3 basic operators (selection, crossover and mutation). The optimization process used by the GA follows the next steps: The GA generates individuals as possible solutions. These individuals are encoded in two vectors of real numbers which represent amplitudes and phase perturbations. Each individual generates an array factor of certain characteristics of side lobe level and directvity. Then, the genetic operators of selection, crossover and mutation are used. GA evolves the individuals to a global solution that generates an array factor with minimum side lobe level and maximum directivity in the direction of interest.

In this work, the GA is used just as an optimization tool for the advantages of the algorithm itself. The performance comparison between GA and others algorithms in this application is outside the scope of this paper.

Finally, the objective function (Of) we want to minimize can be written as:

$$Of = \min[(|AF(\theta_{SLL}, \varphi_{SLL}, \mathbf{a})|/\max|AF(\theta, \varphi, \mathbf{a})|) + (1/D(\theta, \varphi, \mathbf{a}))] \quad (7)$$

where $(\theta_{SLL}, \varphi_{SLL})$ is the angle where the maximum side lobe is attained. The goal is to minimize the weighted sum that involves both objectives (side lobe level and directivity), which are uniformly weighted in the cost function.

3. SIMULATION SETUP AND RESULTS

3.1. Case Study

To analyze the performance of a multi-beam CORPS-BFN in a planar antenna array. We proposed a configuration capable of controlling 9 orthogonal beams simultaneously. In the same way, taking advantage of unique features of CORPS technology we proposed a novel way to feed the network for the planar array. In this proposal, the control of the 9 beams is realized by alternating input ports in subgroups

where the input ports are reused by more than one signal or beam as illustrated in Fig. 2.

The CORPS feeding network system was established defining the structure of CORPS-BFN system in 2 stages to feed the planar array. Each stage is composed of N CORPS-BFN blocks of one-dimension. These blocks are collectively integrated into a complete CORPS-BFN system (2D CORPS-BFN), shown in Fig. 2.

The first stage is formed by 8 CORPS-BFN blocks of one dimension with 15 input ports and 16 output ports. The index in each input port, shown in Fig. 2, indicates the number of beams or signals introduced, related with a group of complex inputs for each beam, i.e., the index number 1 of each CORPS-BFN block belongs to the group of complex inputs for the beam #1 and so on for the 9 beams (the asterik denotes that the index input is not excited).

The second stage is formed by 16 CORPS-BFN blocks of one dimension with 8 input ports and 9 output ports. The 8 input ports of each of the 16 CORPS-BFN blocks in this stage are connected to the 16 output ports of each of the 8 CORPS-BFN blocks of the first stage. The stages are connected as follows. The 8 input ports of the first CORPS-BFN block in the second stage are connected to the first output of each of the 8 CORPS-BFN blocks of the first layer, and the 8 input ports of the second CORPS-BFN block in the second stage are connected to the second output of each of the 8 CORPS-BFN blocks of the first stage and so on for all CORPS-BFN blocks in the second stage. Furthermore, as shown in Fig. 2, the input index of each CORPS-BFN block of the second stage is determined by the index of the CORPS-BFN block of the first stage, e.g., the 2nd input port of

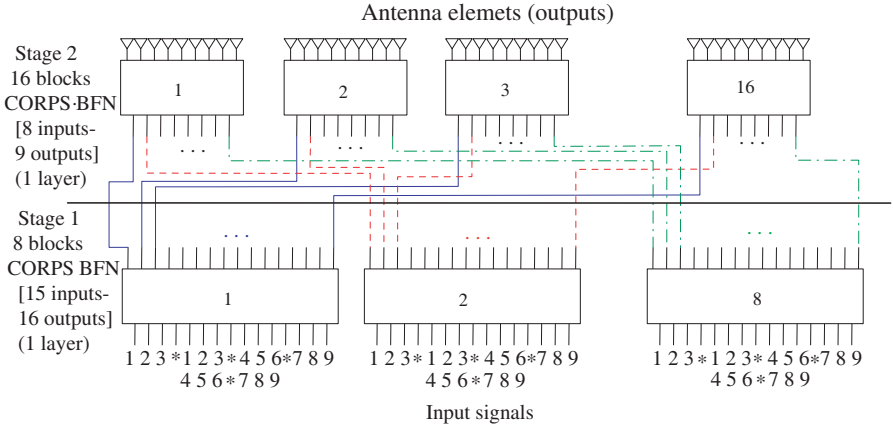

Figure 2. Network configuration of the CORPS-BFN system.

the 1st CORPS-BFN block of the second stage is connected to the 1st output port of the 2nd CORPS-BFN block of the first stage.

In the CORPS-BFN system shown in Fig. 2, there are a total of 144 outputs after the second stage feeding a planar array of 12×12 antenna elements as shown below in Fig. 3.

The planar array structure in Fig. 3 is fed by the network described above. The complete multi-beam system is designed to generate 9 orthogonal beams simultaneously. This multibeam system design is achieved through the reuse of input ports for more than one beam together with the natural overlap between adjacent beams in the CORPS feeding network, to finally obtain an efficient radiating aperture reuse.

In Fig. 3, each beam is formed by a subset of 36 antenna elements (6×6 antenna subarray). The beam #1 is generated by the antenna elements in the bottom left of the array (black square), beam #2 in the bottom center of the array (red square), beam #3 in the bottom right of the array (blue square), beam #4 in the center left of the array (green square), beam #5 in the center of the array (pink square), beam #6 in the center right of the array (purple square), beam #7 in the top left of the array (orange square), beam #8 in the top center of the array (brown square), and beam #9 in the top right of the array (cyan square). Finally, the same Fig. 3 shows the detailed interconnection for beam #1 between the CORPS-BFN blocks of the second stage and the planar array structure. The first 3 rows and columns in the bottom left of the black square (3×3 antenna elements) are the outputs of the first CORPS-BFN block with indices from 1 to 9 (first group of

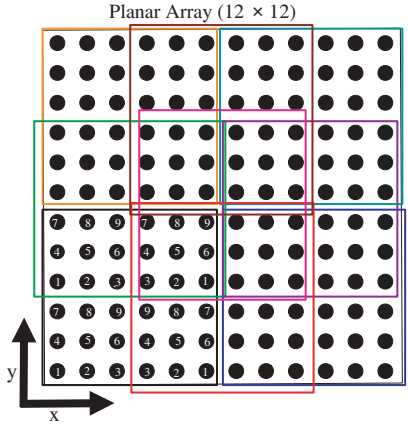

Figure 3. Distribution of the 9 beams within the planar array structure.

outputs). The second group of outputs in the bottom right of the black square are the outputs of the second CORPS-BFN block. The third and fourth groups of outputs in the top of the black square are the outputs of the third and fourth CORPS-BFN blocks, respectively. As shown in Fig. 3, the third and fourth groups of outputs have the same interconnection as the first and second groups of outputs. This interconnection is repeated for each of the 9 beams throughout the planar array structure.

The objective is to evaluate the behavior of the array factor generated by the complete CORPS-BFN system that includes a specific configuration for a multi-beam steerable planar array and demonstrate the possibilities of simplification and the performance advantages of using a CORPS-BFN on a planar array.

The method of GA was implemented to study the behavior of the array factor generated by the configuration shown in Fig. 2. The evaluation of the array factor generated in the azimuth plane in the cut of $\theta = 90^\circ$ considers a steering range of 320° with an angular step of 40° for a planar array of 12×12 antenna elements and a uniform spacing between antenna elements of 0.5λ. We have set the parameters based on our previous experience in solving antenna problems [8, 9]. After a trial and error procedure for parameter tuning, the parameters of the algorithm were set as follows: the GA algorithm is executed using 1000 individuals (population size) through out 1000 iterations to ensure a good sampling of the solution space, with a crossover probability $P_c = 1.0$ and mutation probability $P_m = 0.1$. A selection scheme combining fitness ranking and elitist selection was implemented [7, 14]. The used genetic operators are standard: the well-known two point crossover [7, 14] along with a single mutation where a locus is randomly selected and the allele replaced by a random number uniformly distributed in the feasible region of the search space.

3.2. Simulation Results

Figure 4 shows an example of the array factor of the 9-beam system generated by the CORPS-BFN system presented in Subsection 3.1. The system is a planar array of 12×12 (144) antenna elements and 120 input ports with 16 complex inputs to control 36 antennas for each beam. The optimized radiation pattern shows the CORPS-BFN capabilities to handle SLL and directivity in specific spatial locations for each of the 9 beams. Furthermore, the coherent network can scan each main beam to any desired direction using just 16 input ports for 36 antenna elements. In this specific case, the direction of maximum radiation is directed along the axis φ and set in $\varphi_0 = 20^\circ$ for beam #1, $\varphi_0 = 60^\circ$ for beam #2, $\varphi_0 = 100^\circ$ for beam #3, $\varphi_0 = 140^\circ$

for beam #4, $\varphi_0 = 180°$ for beam #5, $\varphi_0 = 220°$ for beam #6, $\varphi_0 = 260°$ for beam #7, $\varphi_0 = 300°$ for beam #8, and $\varphi_0 = 340°$ for beam #9. Furthermore, in Fig. 5 as a complement to Fig. 4 shows the radiation intensity of the CORPS-BFN system. In this figure, it is easy to observe the main beam steering of each of the 9 beams generated. The specific numerical values of side lobe level, directivity, and amplitude and phase distributions for the array factor illustrated in Fig. 4 are shown in Table 1.

Table 1 shows the numerical values of side lobe level and directivity obtained by simulation, related to specific values in amplitude and phase perturbation distributions for an example of the array factor generated by the 9-beam design of the CORPS-BFN system and illustrated in Fig. 4. The table provides the evaluation of the array factor considering specific directions of maximum radiation previously

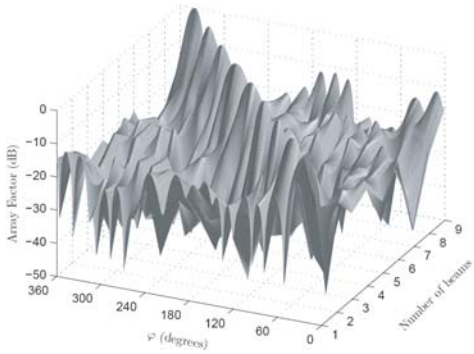

Figure 4. Array factor of the planar array generated by CORPS-BFN system with complex excitations optimized by GA in the cut of 90°.

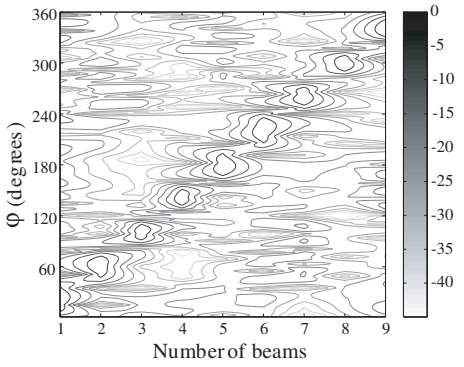

Figure 5. Radiation intensity for each of the 9 beams of the CORPS-BFN system.

Table 1. Numerical values of SLL and D with its amplitude and phase distributions for the array factor shown in Fig. 4.

# of Beam	φ_0 (deg)	SLL(dB)	D(dB)	Amplitude distribution	Phas e distribution(deg)
1	20	-11.94	8.93	10.3970, 7.1140, 5.0772, 2.3355, 5.9640, 4.9668, 9.5763, 3.7475 8.3780, 2.9796, 7.9701, 12.5188, 1.2965, 7.8029, 5.6345, 4.6073	128.52, 96.03, 43.66, 88.50, 150.82, 58.60, 122.73, 103.16, 133.14, 108.33, 85.61, 88.84, 169.88, 110.13, 90.34, 122.43
2	60	-15.24	9.91	11.1752, 1.3147, 11.1378, 9.9898, 11.9785, 12.8518, 7.9790, 4.4019, 9.2311, 12.6083, 4.6889, 13.0916, 3.4131, 13.5388, 6.3963, 10.2621	117.29, 120.53, 71.40, 136.71, 117.41, 99.98, 109.29, 159.27, 108.83, 105.53, 50.00, 54.30, 104.30, 90.13, 105.06, 104.02
3	100	-17.39	11.52	4.7913, 8.8830, 7.9199, 11.5519, 5.7256, 7.1472, 4.8219, 4.1242, 11.9429, 6.9350, 1.9021, 12.1611, 2.6526, 5.5082, 12.2492, 10.4667	84.23, 114.21, 36.61, 44.49, 61.07, 90.34, 113.40, 78.95, 57.26, 78.52, 55.17, 78.27, 95.82, 39.96, 107.12, 79.65
4	140	-17.91	11.31	11.1752, 12.3125, 8.2230, 12.0261, 7.9044, 7.2317, 7.2871, 7.9878, 10.5441, 5.8969, 11.6612, 13.5075, 7.0840, 7.9167, 4.9503, 10.2835	133.67, 66.28, 95.58, 114.76, 79.91, 50.69, 159.68, 89.20, 96.11, 124.97, 127.86, 86.33, 109.82, 102.99, 60.12, 143.35
5	180	-17.63	9.97	8.4864, 6.1150, 5.0772, 8.9706, 4.2146, 13.4937, 7.2871, 4.3038, 10.8085, 3.6832, 12.7302, 8.8640, 3.6862, 13.1437, 7.4750, 2.7377	56.20, 56.72, 49.90, 79.71, 69.81, 54.98, 59.80, 58.67, 58.76, 6.50, 29.78, 64.25, 10.12, 93.02, 19.71, 32.99
6	220	-15.55	9.25	8.4358, 8.7695, 9.2161, 10.9215, 10.0031, 12.1396, 1.9475, 9.8252, 4.6369, 10.8872, 12.0958, 11.0501, 12.1975, 13.9435, 1.1768, 7.5696	104.71, 89.34, 117.21, 102.87, 33.95, 80.82, 21.57, 87.47, 48.68, 78.52, 101.04, 94.33, 128.58, 110.47, 172.19, 110.39
7	260	-14.02	10.46	9.9980, 8.9644, 8.9533, 4.3969, 5.4302, 11.3319, 1.4845, 5.0934, 7.85158, 12.4186, 11.6293, 13.5205, 6.6252, 7.0011, 5.6654, 1.1798	88.01, 124.36, 95.58, 163.43, 73.32, 44.27, 127.69, 89.20, 100.05, 40.12, 112.63, 41.28, 52.71, 50.78, 7.67, 32.99
8	300	-19.07	11.30	12.2955, 0.2421, 11.3812, 7.5728, 5.7256, 10.6813, 9.5463, 2.7598, 10.1114, 4.8048, 7.9727, 4.8329, 9.5378, 5.9465, 13.7190, 4.5325	90.03, 114.21, 66.66, 153.94, 91.44, 91.89, 32.97, 96.85, 133.14, 175.77, 138.22, 125.64, 152.74, 36.72, 82.23, 27.27
9	340	-11.65	10.32	9.4791, 6.4995, 10.8822, 13.4864, 1.9367, 13.7053, 7.7487, 4.3038, 10.3445, 6.1279, 5.8839, 10.7617, 2.4835, 3.3369, 2.2222,9.3555	118.06, 134.68, 109.97, 65.41, 172.05, 126.15, 78.32, 126.13, 113.53, 21.77, 114.16, 106.04, 1.19, 90.01, 141.35, 113.72

defined. In this specific example, the optimization of array factor maintains a low SLL in almost all the scanning range. However, the relation between SLL and D degrades in two further angles from the broadside region [20°, 340°]. Furthermore, note that the orthogonal beams generated and scanned in this example are conformed with just 16 complex inputs and using an aperture of (6×6) 36 elements for each beam.

To perform a deeper analysis of the planar array that considers a CORPS-BFN system as a feeding network, we analyze the tradeoff between side lobe level and directivity on a wide window of visibility over the azimuth plane φ. Figs. 6 and 7 show the performance in side lobe level and directivity for a scanning range between $20° \leq \varphi_0 \leq 340°$, with an angular step of 10°.

The system using the CORPS-BFN under study shows a good performance in the scanning capability over a wide window of visibility

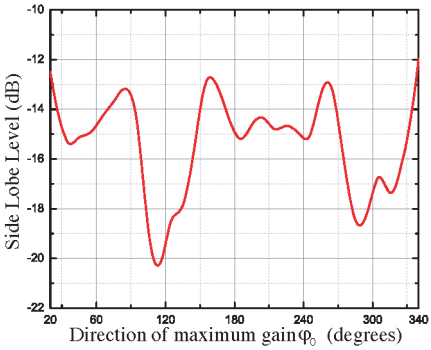

Figure 6. Behavior of the SLL with respect to the direction of interest.

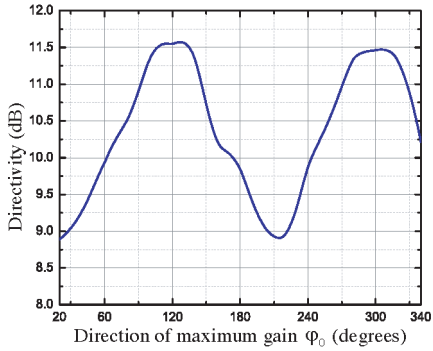

Figure 7. Behavior of the directivity with respect to the direction of interest.

(320°). The complete system behavior generally remains constant throughout the steering range analyzed, i.e., almost constant values of SLL and D in a small window with numeric values approximately between 13 dB to 16 dB for the SLL and 9 to 10.5 for D. Except for two broad regions where higher numerical values are shown for the SLL and D. The first region is located around 120° and the second around 300° approximately (see Figs. 6 and 7).

The above performance is not achieved in linear arrays that use a CORPS-BFN where the scan angle range is small. Also, at angles away from broadside region, these linear arrays show a decreasing behavior in terms of SLL and D, which worsens with the use of a greater number of layers [2, 3]. Although in circular arrays using CORPS-BFN the overall performance (SLL and D) expected would be more constant in all the scanning range, the network simplification is lower than that achieved in this paper for planar array [5].

A specific case to generate nine scannable beams was presented, but it is possible to define different configurations choosing independently the number of antenna elements and the number of input ports (depending on the number of simultaneous orthogonal beams required). In general, it is important to note the significative simplification of the complex inputs. Each of the 9 scannable beams is generated with (N/2)-L complex inputs, i.e., the relationship between the complex inputs, M, and the number of antenna elements, N, for these particular configuration is less than N/2 for each beam (N/2-2 specifically for the proposed configuration). To this simplification of the number of control inputs, we must add the technological advantages offered by CORPS to reuse antenna elements between adjacent beams

(reducing the antenna array aperture) as discussed before. The above improvements offer a substantial simplification of the feeding network.

In this way, the less limited scanning features in a planar array using a CORPS as a feeding network is a better candidate for a greater number of applications based on the scanning capability. Moreover, in this type of scanning applications where the feeding system (including all the associated electronic circuitry) is very complicated, the simplification of the feeding network could be more significant for a planar (bi-dimensional) array.

Although only an example of CORPS-BFN for a planar array based on simulation is presented, depending on the design requirements and needs for a particular application, a more convenient configuration can be easily established and implemented.

4. CONCLUSION

The design of a feeding network based on CORPS technology for scannable multibeam antenna arrays in a planar geometry has been presented. The behavior of the array factor generated by a CORPS-BFN system for a multi-beam steerable planar array was studied and analyzed. Simulation results reveal that the design of CORPS-BFN, which feeds a planar array optimizing the complex inputs with GA, could generate orthogonal and scannable multiple beams with a significant simplification of the beam-forming network. Furthermore, the CORPS-BFN configuration analyzed showed the advantages of adopting this technology in planar arrays for later use in applications requiring multiple simultaneous beams and scanning capabilities.

REFERENCES

1. Betancourt, D. and C. Del Rio Bocio, "A novel methodology to feed phased array antennas," *IEEE Trans. on Anten. and Propag.*, Vol. 55, No. 9, 2489–2494, 2007.
2. Panduro, M. A. and C. Del Rio-Bocio, "Design of beam-forming networks using CORPS and evolutionary optimization," *Int. J. Electron. Commun. (AEU)*, Vol. 63, 353–365, 2009.
3. Panduro, M. A., "Design of beam-forming networks for scannable multi-beam antenna arrays using CORPS," *Progress In Electromagnetics Research*, Vol. 84, 173–188, 2008.
4. Garcia, R., D. Betancourt, A. Ibanez, and C. Del Rio, "Coherently periodic radiation structures (CORPS): A step towards high

resolution imaging systems," *IEEE AP-S 2005*, Washington D.C., 2005.

5. Panduro, M. A., "Simplifying the feeding network for multibeam circular antenna arrays by using CORPS," *Progress In Electromagnetics Research Letters*, Vol. 21, 119–128, 2011.
6. Ferrando, N. and N. J. G. Fonseca, "Investigations on the efficiency of array fed coherently radiating periodic structure beam forming networks," *IEEE Trans. on Anten. and Propag.*, Vol. 59, No. 2, 493–498, 2011.
7. Rahmat-Samii, Y. and E. Michielssen, *Electromagnetic Optimization by Genetic Algorithms*, Wiley-Interscience, New York, 1999.
8. Arce, A., D. H. Covarrubias, and M. A. Panduro, "Performance evaluation of population based optimizers for synthesis of linear antenna arrays," *Proc. of the 6th IASTED Int. Conf.*, Vol. 649, 044–103, 2011.
9. Reyna, A. and M. A. Panduro, "Optimization of a scannable pattern for uniform planar antenna arrays to minimize the side lobe level," *Journal of Electromagnetic Waves and Applications*, Vol. 22, No. 16, 2241–2250, 2008.
10. Xu, O., "Collimation lens design using AI-GA technique for gaussian radiators with arbitrary aperture field distribution," *Journal of Electromagnetic Waves and Applications*, Vol. 25, No. 5–6, 743–754, 2011.
11. Fernandez-Delgado, M., J. A. Rodriguez-Gonzalez, R. Iglesias, S. Barro, and F. J. Ares-Pena, "Fast array thinning using global optimization," *Journal of Electromagnetic Waves and Applications*, Vol. 24, No. 16, 2259–2271, 2010.
12. Liu, Y., X. Chen, and K. Huang, "A novel planar printed array antenna with SRR slots," *Journal of Electromagnetic Waves and Applications*, Vol. 24, No. 16, 2155–2164, 2010.
13. Siakavara, K., "Novel fractal antenna arrays for satellite networks: Circular ring Sterpinski carpet arrays optimized by genetic algorithms," *Progress In Electromagnetics Research*, Vol. 103, 115–138, 2010.
14. Goldberg, D. E., *Genetic Algorithms in Search, Optimization and Machine Learning*, Addison-Wesley, Massachusetts, 1989.
15. Balanis, C. A., *Antenna Theory: Analysis and Design*, Wiley-Interscience, New Jersey, 2005.